Environmental Science & Technology

pubs.acs.org/est

Article

Tiered Leak Detection and Repair Programs at Simulated Oil and Gas Production Facilities: Increasing Emission Reduction by Targeting High-Emitting Sources

Felipe J. Cardoso-Saldaña*

Cite This: *Environ. Sci. Technol.* 2023, 57, 7382−7390

Read Online

ACCESS | Metrics & More | Article Recommendations | Supporting Information

ABSTRACT: Distributions of methane emission rates originating from oil and gas production facilities are highly skewed and span 6−8 orders of magnitude. Traditional leak detection and repair programs have relied on surveys with handheld detectors at intervals of 2 to 4 times a year to find and fix emissions; however, this approach may lead unintended emissions to be active for the same interval independently of their magnitude. In addition, manual surveys are labor intensive. Novel methane detection technologies offer opportunities to further reduce emissions by quickly detecting the high-emitters, which account for a disproportionate fraction of total emissions. In this work, combinations of methane detection technologies with a focus of targeting high-emitting sources were simulated in a tiered approach for facilities representative of the Permian Basin, a region with skewed emission rates where emissions above 100 kg/h account for 40−80% of production site-wide total emissions, which include sensors on satellites, aircraft, continuous monitors, and optical gas imaging (OGI) cameras, with variations on survey frequency, detection thresholds, and repair times. Results show that strategies that quickly detect and fix high-emitting sources while decreasing the frequency of OGI inspections, which find the smaller emissions, achieve higher reductions than quarterly OGI and, in some cases, reduce emissions further than monthly OGI.

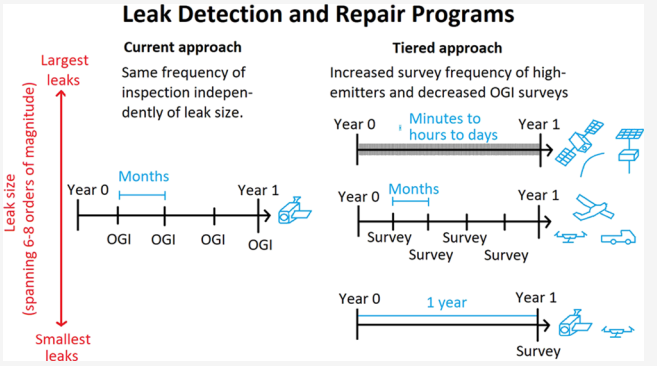

KEYWORDS: *leak detection and repair, methane emissions, greenhouse gas emissions, oil and gas, super-emitter*

INTRODUCTION

Methane is a potent greenhouse gas which exerts the second largest climate forcing after carbon dioxide.[1] Rapid reductions on methane emissions are needed to limit global warming to 1.5 °C. As such, in 2021, nations around the globe signed the Global Methane Pledge, committing to reduce their collective methane emissions 30% from 2020 levels by 2030.[2] Atmospheric methane has multiple natural and anthropogenic origins, with activities from coal mining and oil and natural gas systems accounting for ∼18% of global emissions for the year 2017.[3] Emissions from oil and natural gas systems are seen as the sector that can account for the majority of emission reductions by 2030, and many companies have set targets for emission reduction.[4]

Multiple studies performed over the last decade have improved the knowledge of emissions occurring along oil and gas supply chains and have shown that emission distributions are highly skewed,[5,6] with a few number of sources accounting for a large fraction of emissions (high-emitters). The variation of emission rates can be significant with emission rates spanning 6 to 8 orders of magnitude (Figure 1a).[7,8] Emission rates reported from these studies are snapshots; however, absolute emissions are given by the time an emission is active and by its emission rate. One strategy to reduce emissions from oil and gas activities is through mitigation of unintended emissions in leak detection and repair (LDAR) programs, which shorten their active time.

The highest methane emission rate reported by Allen et al.,[7] in a study that sampled production sites in multiple basins with optical gas imaging (OGI) cameras, was 5.5 kg/h (Figure 1a). If this leak was active for 91 days (half of the time between two times a year LDAR inspections), it would release the same amount of methane that the highest emission rate from a study surveying the Permian Basin using aircraft-based measurements[8] would if it was active for less than an hour (Figure 1b). Thus, high emission rates active for a relatively short amount of time can have a significant impact on total emissions, so they should be detected and fixed quickly.

Received: November 15, 2022
Revised: March 10, 2023
Accepted: March 31, 2023
Published: May 2, 2023

https://doi.org/10.1021/acs.est.2c08582
Environ. Sci. Technol. 2023, 57, 7382−7390

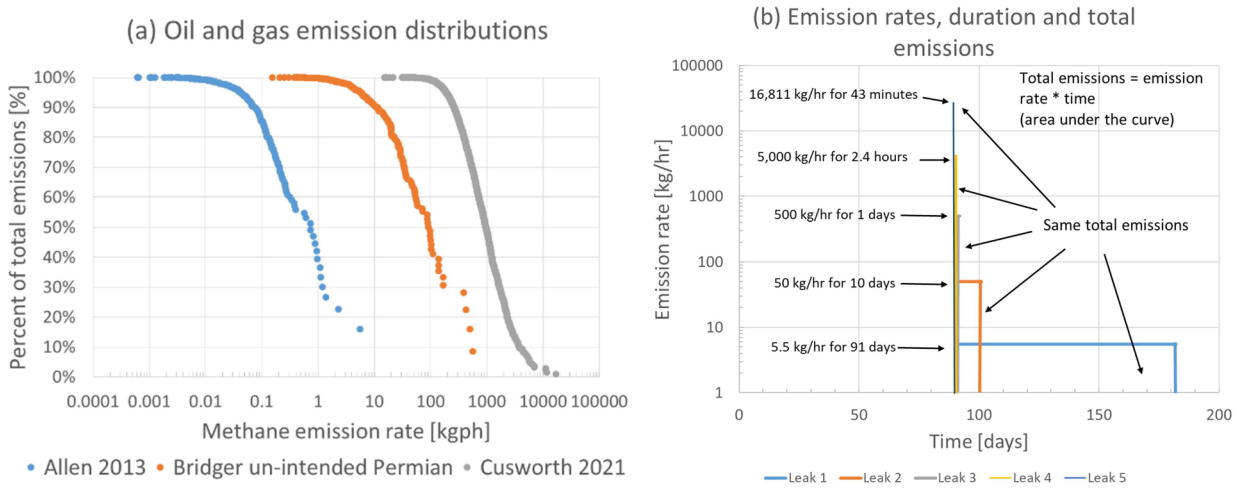

Figure 1. (a) Emission distributions from oil and gas infrastructure and (b) same total emissions for various emission rates and durations. The detection threshold of OGI cameras used in Allen et al.[7] is ∼0.001−0.01 kg/h, the detection threshold of Bridger is ∼1−3 kg/h, and the detection threshold of the flyovers from Cusworth et al.[8] is ∼10−20 kg/h.

Traditionally, LDAR programs have relied on OGI or method 21 with inspections 2 or 4 times a year, depending on the type of facility, as currently allowed by federal regulations.[9] Under this approach, the time between surveys has been independent of the size of leaks, leading to leaks with high emission rates to potentially be active for large amounts of time before they are found. However, in recent years, there have been rapid advancements in technologies to detect methane with sensor platforms, including aircraft, satellites, drones, trucks, and fixed monitors or cameras on pads, offering opportunities for LDAR programs that achieve greater emission reductions and that are less labor intensive than conventional approaches.[10]

In order to compare the reduction in emissions between LDAR programs, computational models such as the fugitive emissions abatement simulation toolkit (FEAST)[11] or LDAR-Sim[12] have been developed. With these models, it has been demonstrated that novel technologies can achieve at least the same reduction as 2 or 4 times a year OGI[13] and that OGI inspections are still needed in follow-up repairs from the novel technologies to locate the detected emissions and verifying their presence in addition to finding the smallest leaks. However, studies that employ these models have not evaluated combinations of multiple technologies besides aerial + OGI, nor continuous monitors. In addition, these studies have simulated facilities with the same equipment and components, while the types of equipment can vary depending on their vintage and throughput.

Multiple studies have shown that emissions from oil and gas activities are larger than reported emissions, and the discrepancy is attributed to large unintended emissions.[14,6] There is a need to achieve emission reductions in a way that is effective and safe as frequent inspections using manual OGI cameras require extensive driving between facilities. This work will assess whether targeting high-emitting sources quickly achieves higher reduction than conventional programs at intervals of months by layering methane detection technologies with different detection thresholds and survey frequencies. The facilities simulated are heterogeneous to understand the effect of having certain LDAR programs with more frequent surveys present only at facilities with larger potential to emit. The effect of varying repair times for large emissions is also evaluated. The emission distributions are representative of the Permian Basin, an oil and gas production basin with large contribution from emissions above 100 kg/h (40−80% of production site-wide total emissions).[8,15−17]

METHODOLOGY

This work uses a model based on the leak module of the methane emission estimation tool (MEET)[18,19] with the inclusion of LDAR programs. The resulting model is similar in operation to other open source LDAR models[11,12] but has some differences that are detailed in the following sections. The simulation is stochastic, and each LDAR scenario was ran in a Monte Carlo approach 50 times to estimate the 95% confidence interval on the mean reduction. The temporal resolution of the simulation was 1 day and was ran for a period of 5 years.

Facilities. The facilities simulated here consist of tank batteries taken from Stokes et al.[20] (priority sites) in addition to wellhead-only sites (non-priority sites). Tank batteries include small tank batteries, based on the number of tanks, which are representative of older facilities and typically include one or a few wellheads, separation equipment, and tanks on the same pad. Tank batteries also include centralized tank batteries which have larger numbers of tanks and typically do not have wellheads on the pad, rather they process output from multiple wellhead-only sites located at pads in close proximity. The types of facilities here simulated are the first difference compared to previous simulations.[11,12] Details on equipment and component counts at each facility are described in the Supporting Information (SI) Section S1.

Emission Measurements. One of the most important parameters in LDAR models is the emission distribution, which needs to be representative of the conditions in the field, for example by including high-emitters. Here, the approach was not to fit a distribution to the data and rather sample from measurements as done in Zavala-Araiza et al.[14] and Allen et al.[21] Only non-routine (unintended) emissions were simulated as the objective was to estimate emission reduction; these emissions constitute part of the total emissions at oil and gas facilities which also include sources that occur by design.

Here, two different sources of emissions based on field data were combined to have a representative emission distribution of the Permian Basin. The first data set came from studies using close-range inspections (OGI cameras or method 21) from

https://doi.org/10.1021/acs.est.2c08582
Environ. Sci. Technol. 2023, 57, 7382−7390

Allen et al.,[7] Bell et al.,[22] and Kuo et al.[23] as described by Kemp and Ravikumar[13] with the addition of data from Pacsi et al.[24] These studies were chosen as they have information of the equipment where each emission originated from, which was used to randomly assign emissions in this study from that equipment category, for example a component at a separator will sample from the emissions originating from separators from the combined data sets. The second data set was from Permian Basin flyovers from Bridger Photonics, whose distribution is shown in Figure 1 and was also disaggregated by equipment. This data set includes measurements that are higher than 100 kg/h, which is the definition of a super-emitter (high-emitter) event proposed by the Environmental Protection Agency (EPA).[25] Bridger Photonics uses a continuous wave LiDAR measurements and has been described and evaluated by Johnson et al.[26] and Conrad et al.[27] Only the emissions where operators confirmed that the source was non-routine, after following-up, were included in the distribution except for flares whose emission rates were taken directly from measurements while their fraction with unintended emissions was taken from third party data (see below). The term non-routine is used interchangeably with leak in the text. Sensitivity analysis S0 was performed by adding to the distribution of close-range inspections data from Eastern Research Group (ERG)[28] and Ravikumar et al.,[29] as described by Kemp and Ravikumar[13] and assigning emissions randomly from a combined distribution, independently of which equipment the data came from, except for tanks and flares where the data come from the flyover distribution.

Emissions from the studies using close-range inspections were added to the flyover data set, which had 1251 site surveys, to account for emissions below the detection threshold of the aerial flyovers and within the partial detection range of the aerial flyovers (see SI Section S2 for details). The first step to integrate these measurements was to average the percentage of sites with emissions in each close-range study, weighting the average based on the number of sites surveyed in each study. The weighted average resulted in 71% of sites having leaks from the close-range inspection data sets. This value carries uncertainty as it aggregates field studies performed in different locations with different types of facilities and at different times and, thus, this value was varied in sensitivity analyses S1 and S2 to be 91 and 51%, respectively, to assess the effect of this parameter on the emission reduction results. For additional details of combining the close-range inspection emissions with the flyover data set, see SI Section S2.

Leak Generation Rates. Transitions between leaking and non-leaking states were simulated with the same equations (eqs 1−3) as in the MEET model.[18,19] Non-routine emissions from tanks and flares were also simulated with these equations, and they were modeled at the equipment level, whereas emissions from the other equipment were modeled at the component level.

$$t_{\text{next leak starts}} = t_{\text{previous leak stops}} - \text{MTBF} * \text{Ln}(1 - \text{random number}) \quad (1)$$

$$t_{\text{leak stops,no LDAR}} = t_{\text{leak start}} - \text{MTTR} * \text{Ln}(1 - \text{random number}) \quad (2)$$

$$\text{MTTR} = \left(\frac{\text{pLeak}}{1 - \text{pLeak}}\right) * \text{MTBF} \quad (3)$$

where pLeak is the fraction of a particular component or equipment that are observed to be emitting in a given point in time based on field studies. Mean time between failures (MTBF) is the average time it takes for a new leak to emerge and is estimated based on field data; this variable is referred to as leak generation rate in FEAST and LDAR-Sim. Mean time to repair (MTTR) represents the time that leaks stop emitting outside LDAR inspections and is a parameter referred to as null repair rate in FEAST and LDAR-Sim.[11,12] The random number is drawn from a uniform distribution between 0 and 1. MTTR is included in these types of models as it keeps the number of leaks relatively steady at the value of pLeak, when averaged over a long period of time and over multiple simulations, in scenarios that do not have LDAR programs.

From the variables in eqs 1−3, pLeak can be directly obtained from surveys, MTBF is typically estimated based on surveys, and MTTR is then estimated based on eq 3. The way that MTBF is typically estimated is to count the number of components of a particular kind that are leaking on a given LDAR survey and then divide the total time those components were operating in between LDAR surveys by the number of leaks to arrive at the average time to leak.[12] The MTTR and MTBF parameters for component type of leaks were taken directly from the MEET model, while MTTR and MTBF for emissions from tanks and flares were estimated using the same approach as components based on the time between the first Bridger flyover and the second one. Because some sites had OGI inspections in between the aerial surveys, if a site had detected emissions during an OGI inspection (some tanks were found to be emitting), those findings were also counted in the number of emissions in the time frame as they were repaired before the second Bridger flyover. The pLeak value used for tanks was from the first aerial surveys as this is the baseline. For flares, the pLeak was taken from aerial surveys from the Environmental Defense Fund's PermianMap,[30] which reports that 10% of flares in the Permian are malfunctioning, including half of the malfunctioning as unlit. At the beginning of the simulation, the pLeak number of each component or equipment was assigned to determine which components and equipment were emitting initially. Table 1 shows the values of pLeak, MTBF, and MTTR used for the base case simulations which are default values from the MEET model for components.[18,19] MTBF and MTTR are mean values that will lead to temporal variability of individual leaks based on eqs 1 and 2. Figure S4 shows a distribution of times for leak onset and times before leaks stop in the absence of LDAR to illustrate the temporal variation.

Table 1. Parameters Used in Base Case Scenarios for Transition between Leaking and Non-leaking States

component/equipment	pLeak	MTBF [days]	MTTR [days]
valves	0.00191	191,132	366
connectors	0.000665	548,968	365
open ended lines	0.00646	56,536	368
pressure relief valves	0.0272	13,398	375
flanges	0.000665	548,968	365
other	0.000665	548,968	365
tanks	0.046	1515	73
flares	0.1	1435	159

Leak generation rates and null repair rates (MTBF and MTTR) are among the parameters with the most uncertainty and also ones that affect outcomes the most.[12,13] To account for

https://doi.org/10.1021/acs.est.2c08582
Environ. Sci. Technol. 2023, 57, 7382−7390

Table 2. Parameters Varied in Sensitivity Analyses and Base Case Simulations

set of simulations	close-range inspection data sets, which are then combined with the flyover data set	fraction of sites with emissions from close-range inspections when combining close-range and flyover data sets at each Monte Carlo iteration	pLeak[a]	MTBF [days][a]	MTTR [days][a]
base case	Allen et al.,[7] Bell et al.,[22] Kuo et al.,[23] and Pacsi et al.[24b]	0.71	tanks = 0.046; flares = 0.1	tanks = 1515; flares = 1435	tanks = 73; flares = 159
sensitivity analysis S0	Allen et al.,[7] Bell et al.,[22] Kuo et al.,[23] Pacsi et al.,[24] ERG,[28] and Ravikumar et al.[29c]	0.71	tanks = 0.046; flares = 0.1	anks = 1515; flares = 1435	tanks = 73; flares = 159
sensitivity analysis S1	Allen et al.,[7] Bell et al.,[22] Kuo et al.,[23] and Pacsi et al.[24b]	0.91	tanks = 0.046; flares = 0.1	anks = 1515; flares = 1435	tanks = 73; flares = 159
sensitivity analysis S2	Allen et al.,[7] Bell et al.,[22] Kuo et al.,[23] and Pacsi et al.[24b]	0.51	tanks = 0.046; flares = 0.1	anks = 1515; flares = 1435	tanks = 73; flares = 159
sensitivity analysis S3	Allen et al.,[7] Bell et al.,[22] Kuo et al.,[23] and Pacsi et al.[24b]	0.71	tanks = 0.046; flares = 0.1	tanks = 103.7; flares = 45	tanks & flares = 5
sensitivity analysis S4	Allen et al.,[7] Bell et al.,[22] Kuo et al.,[23] and Pacsi et al.[24b]	0.71	tanks = 0.046; flares = 0.1	tanks = 207.4; flares = 90	tanks & flares = 10
sensitivity analysis S5	Allen et al.,[7] Bell et al.,[22] Kuo et al.,[23] and Pacsi et al.[24b]	0.71	tanks = 0.046; flares = 0.1	tanks = 622.2; flares = 270	tanks & flares = 30

[a]All sets of simulations use the pLeak, MTBF, and MTTR parameters specified in Table 1 for: valves, connectors, open ended lines, pressure relief valves, flanges, and other components. [b]Emissions assigned based on equipment type from measurements for all sources. [c]Emissions assigned independently of equipment type from measurements except for tanks and flares.

the uncertainty in their values, Fox et al.[12] suggest performing sensitivity analyses varying these parameters. In this work, sensitivity analyses were constructed based on empirical data on duration of emissions from Cusworth et al.,[8] which surveyed facilities multiple times in the Permian in 2019 for a month and a half period to assess persistency of high-emitters. To be able to use eqs 1−3, the traditional approach is to get pLeak from surveys, estimate MTBF from survey data, and calculate MTTR using eq 3. Here, the approach was to first estimate MTTR values based on empirical data on emission duration from Cusworth et al.[8] followed by calculation of MTBF values using eq 3 and the pLeak values from surveys. A description of how these parameters were derived is detailed in SI Section S3, and the values varied across the sensitivity analyses are shown in Table 2. Each leaking event is assumed to be independent of each other at a given source and has the same recurrence rate (i.e., same MTBF) independently of how many times it has been repaired after being observed in LDAR surveys, which means that absolute reductions shown in the results section represent a lower bound.

LDAR Scenarios. In this work, multiple combinations of technologies with various levels of detection thresholds were used. Initially, the simulations were performed using the base case parameters. In addition, all scenarios were performed again for the various sensitivity analyses (S0−S5).

The first scenario was no LDAR, that serves as a baseline to which the LDAR scenarios were compared to, in order to estimate reduction; the first year of each simulation was not included when estimating reduction, only years 2−5 were included. Scenarios with only OGI surveys were included with frequencies of 1× (one time a year), 2×, 4×, 6×, and 12× with a detection threshold taken from Zimmerle et al.[31] assuming high experience of operators. The 4× OGI scenario corresponds to the survey frequency proposed by EPA for new regulations, for facilities with more than one piece of equipment on site besides wellheads,[32] and was used as reference.

Aerial scenarios were simulated in combination with OGI by having in a given year one scheduled OGI inspection at all facilities plus 1×−11× aerial surveys. For example, 1× aerial + 1× OGI means two inspections a year that are 6 months apart from each other, one using aerial and one using OGI. The detection thresholds simulated for aerial were: 2, 5, 10, and 25 kg/h. Scenarios with combinations of satellite + aerial + OGI were included by having the same scenarios described for aerial + OGI, plus the satellite coverage. For satellites, two survey frequencies that cover all facilities were included, daily revisit and weekly revisit; while these revisit frequencies might not be currently available, multiple satellite constellations are being planned which will enable them.[33,34] The two satellite detection thresholds included were 50 and 100 kg/h, which are within the range of what Jacob et al.[33] described as the capabilities of point source monitoring satellites. Scenarios with satellites + 1× OGI and no aircraft were also included. Satellite detection of emissions is diminished by cloud cover, and details of how its effect was implemented in the model are described in SI Section S4.

Continuous monitoring sensors were included using networks of sensors: one or less than one sensor per site combined with OGI 1×. Based on simulated data from Chen et al.,[35] it was assumed that these networks of sensors were able to detect emissions of 5 and 10 kg/h within 1 week of emission onset (uniform distribution, sample randomly the number of days to detection). Additional scenarios were included that add satellite detection in parallel with the networks of continuous monitors + OGI.

Continuous monitors were also simulated as being present on a site basis combined with OGI 1×. It was assumed that all sites had sensors and emissions were detected within 1 day of onset. The detection thresholds simulated were 0.2, 2, 5, and 10 kg/h. Additional scenarios were included that add satellite detection on top of the continuous monitors + OGI.

Finally, a prioritized approach was used with site level continuous monitors present only on tank batteries (priority sites), which have tanks and/or flares, since they are the most common sources of high-emitters, while wellhead-only sites (non-priority sites) were not assigned continuous monitors. The priority sites had continuous monitors + 1× OGI, while the non-priority sites had scenarios of 1× OGI, and 1−5× aerial + 1× OGI. Scenarios with satellites in parallel with the described sensors were also included. Table S2 shows in detail the scenarios simulated.

Repair Times. Once leaks were found by the detection technologies, they were scheduled for repair. For OGI inspections, repair times were selected at random from a uniform distribution between 1 and 30 days after inspections. For aerial inspections, repair times were randomly selected

https://doi.org/10.1021/acs.est.2c08582
Environ. Sci. Technol. 2023, 57, 7382−7390

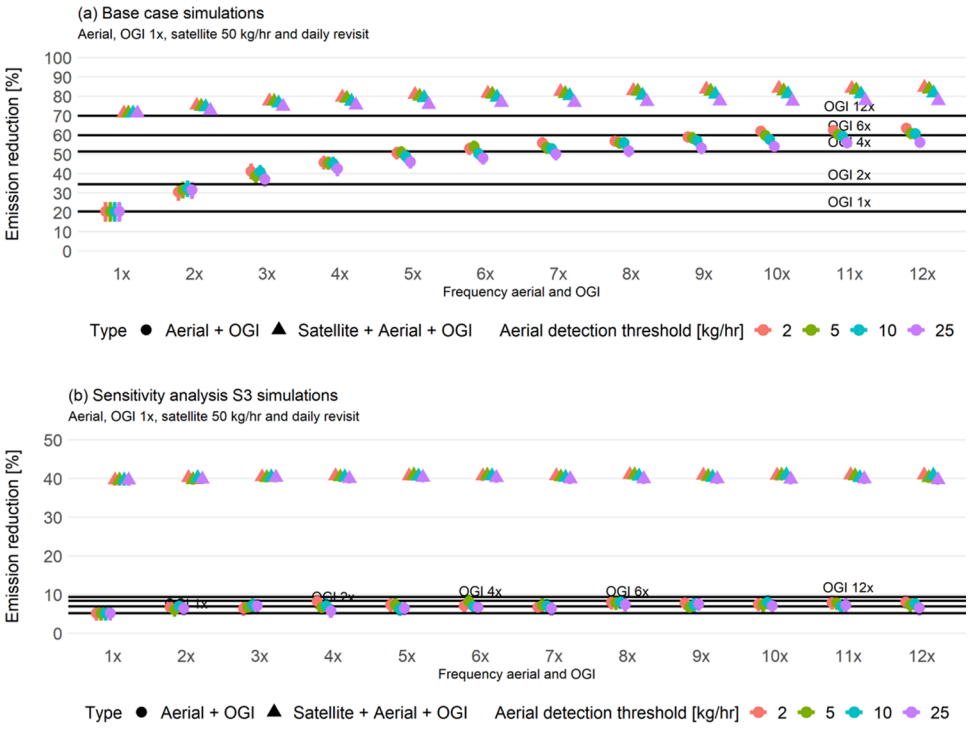

Figure 2. Emission reduction of LDAR scenarios with aerial + OGI and satellite + aerial + OGI for (a) base case (long duration of high-emitters) and (b) sensitivity analysis S3 (short duration of high-emitters) scenarios. The color represents the detection threshold of the aerial technology. Horizontal black lines indicate the reduction of OGI-only LDAR programs. The horizontal axis represents the frequency of aerial and OGI; OGI is used only once a year in all scenarios, so the variation on frequency is due to the aerial surveys.

between 1 and 30 days after follow-up to the sites was done, which was assumed to be 1−14 days after the site's flyover. Leaks found with satellites were assumed to be repaired within 2 days. Leaks detected with continuous monitors and greater than 10 kg/h were assumed to be repaired within 7 days, while those equal to or below this threshold within 30 days. When surveys from different technologies coincided on the same day (e.g., satellite and aircraft) and if the leak was found by more than one technology, the lowest repair time was chosen. Additional scenarios included having leaks detected by satellites and continuous monitors, repaired within 30 days, as opposed to sooner, to compare the effect of varying repair times on the emission reduction.

In total, based on the permutations of detection threshold and repair times, 566 simulations were ran for the base case in addition to 566 for each of the sensitivity analysis S0−S5 (see Tables 2 and S2 for details of simulations ran). Technologies such as aerial, continuous monitors, and satellites need a follow-up to find the exact cause of the leak and repair it, and while being at the site operators might survey parts or the entire facility to find additional potential leaks. Here, it was assumed that only the emissions found in the original surveys were repaired as a conservative approach. Reduction is estimated by comparing emissions of a given LDAR program to a simulation without LDAR; if the time that a leak is active is not decreased, due to an LDAR program, from the time that it would have stopped emitting based on its MTTR, there is no reduction gain.

LDAR SIMULATION RESULTS

The following sub-sections focus on comparing emission reductions of particular combinations of technologies with respect to OGI, starting with episodic surveys (satellite, aerial, and OGI), followed by combinations with continuous monitors. SI Section S6 analyzes the effect on emission reduction of including vs not including emissions from flares; and given that there is no significant difference on a relative or absolute basis, results including emissions from flares are reported in following sub-sections. SI Section S7 assesses the change in reduction of the sensitivity analyses compared to the base case simulations, and it shows that the most sensitive parameters are the leak generation and null repair rates. Results reported in following sub-sections include base case and sensitivity analysis S3 simulations to contrast results since they have the longest and shortest duration of high-emitters, respectively.

Combinations of Satellite, Aerial, and OGI Sensors. The emission reduction of aerial surveys under various detection thresholds with yearly OGI is shown in Figure 2. As has been reported previously, emissions decrease with increasing frequency of inspections; however, the benefit of additional inspections has diminishing returns.[13] Ravikumar[36] estimated that LDAR programs consisting of 6× aerial with yearly OGI, having detection thresholds of 1 and 11.6 kg/h for aerial technologies, achieve higher reductions than OGI 4× in scenarios with high-emitters of long duration in line with the results shown here. Per Figure 2, having a lower detection threshold helps aerial technologies to achieve higher reductions, particularly in scenarios of long-duration of high-emitters (Figure 2a) as the number of flyovers per year increases. By contrast, in scenarios with short duration of high-emitters (Figure 2b), the detection threshold of aerial technologies is not very sensitive.

Figure 2 also includes a tiered approach with daily satellite revisits having a detection threshold of 50 kg/h plus the aerial and OGI surveys. The addition of satellite-based detection leads to substantial reductions in emissions as all scenarios that include satellite surveys achieve more reductions than even

https://doi.org/10.1021/acs.est.2c08582
Environ. Sci. Technol. 2023, 57, 7382−7390

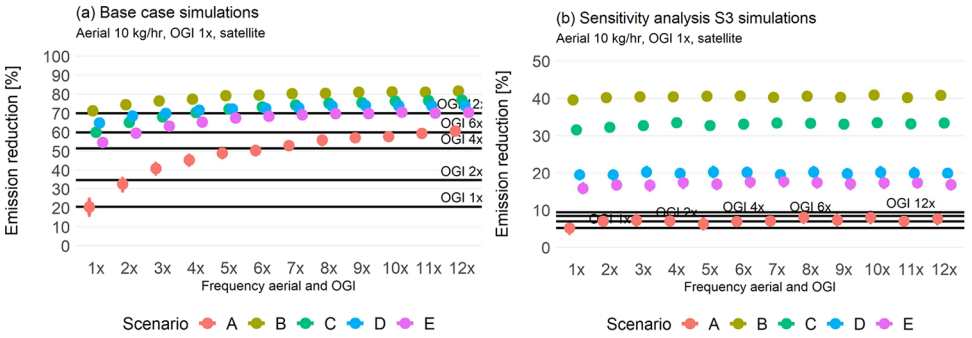

Figure 3. Emission reduction of LDAR scenarios with satellite + aerial + OGI for (a) base case (long duration of high-emitters) and (b) sensitivity analysis S3 (short duration of high-emitters) simulations. Scenario A is no satellite. Scenario B is satellite with 50 kg/h and daily revisit times. Scenario C is satellite with 100 kg/h and daily revisit times. Scenario D is satellite with 50 kg/h and weekly revisit times. Scenario E is satellite with 100 kg/h and weekly revisit times. Horizontal black lines indicate the reduction of OGI-only LDAR programs. The horizontal axis represents the frequency of aerial and OGI; OGI is used only once a year in all scenarios, so the variation on frequency is due to the aerial surveys.

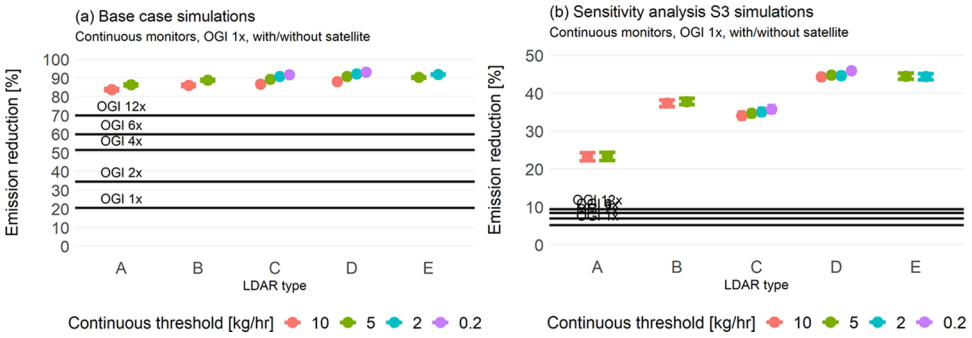

Figure 4. Emission reduction of LDAR scenarios with continuous monitoring + OGI with/without satellite for (a) base case (long duration of high-emitters) and (b) sensitivity analysis S3 simulations (short duration of high-emitters). LDAR type A is networks of sensors + 1× OGI. LDAR type B is networks of sensors + satellite with 50 kg/h detection threshold and daily revisits + 1× OGI. LDAR type C is continuous monitors at all sites + 1× OGI. LDAR type D is continuous monitors at all sites + satellite with 50 kg/h detection threshold + 1× OGI. LDAR type E is continuous monitors only at tank batteries + satellite with 50 kg/h and daily revisits at all facilities + 1× OGI at all facilities. Horizontal black lines indicate the reduction of OGI-only LDAR programs. The color indicates detection thresholds of the continuous monitoring sensors.

monthly OGI. This reduction occurs because of the skewness in the emission distribution where high-emitters account for a disproportionate share of total emissions and by having a strategy to prioritize detection and repair of the high-emitters. In summary, significantly higher reductions can be achieved with tiered approaches that include frequent inspections of satellites in parallel to the aerial + OGI surveys as opposed to more frequent aerial surveys with a lower detection threshold plus OGI. The effect of repair times is discussed in SI Section S9.

Effect of Satellite Frequency and Detection Threshold. Figure 3 shows the emission reductions of LDAR programs that include satellite, aerial, and OGI technologies with variation in satellite survey frequency and detection threshold. In scenarios with long duration of high-emitters (Figure 3a), all combinations perform better than 4× OGI and some scenarios better than 12× OGI, particularly as the frequency of aerial surveys increases. In scenarios of short duration of high-emitters (Figure 3b), all combinations that include a satellite perform better than 12× OGI although the reduction is significantly higher for those with daily revisits compared to those with weekly revisits, suggesting that satellite survey frequency is the most important parameter followed by detection threshold.

Combinations of Continuous Monitors with Satellite and OGI Sensors. All types of LDAR scenarios with continuous monitoring, whether present at all sites, present only on tank batteries (higher potential to emit) or as networks of sensors (fewer sensors per site and longer detection times) achieve a higher reduction than 12× OGI (Figure 4), independently of the duration of high-emitters. In scenarios of long durations of high-emitters, the differences between the various scenarios of continuous monitors are relatively small; however, the difference becomes larger as the duration of short-emitters decreases. Here, scenarios that include a layer of satellite detection with daily revisits achieve higher reduction than those with only the continuous monitors and OGI as it is assumed that emissions detected with satellites are fixed within 1−2 days, while those detected with continuous monitors and above 10 kg/h are fixed within 7 days (LDAR types B vs A and D vs C of Figure 4). Thus, the time to repair high-emitting sources can also play an important role in further decreasing emissions (see SI Section S9 for more details). Higher reductions can be achieved as the detection threshold of continuous monitors decreases although the difference is relatively small (LDAR types C and D of Figure 4), suggesting that LDAR strategies that focus on quickly finding and fixing emissions larger than 10 kg/h are effective, due to the skewness in the emission distributions, and emissions below this threshold can be detected in the yearly OGI.

Scenarios with site level continuous monitoring sensors across all sites result in larger reductions on emissions than networks of sensors in scenarios of short duration of high-emitters (LDAR types C vs A and D vs B, on Figure 4b). However, reductions achieved by having only continuous monitoring on priority sites are comparable to those having them across all sites (LDAR

https://doi.org/10.1021/acs.est.2c08582
Environ. Sci. Technol. 2023, 57, 7382−7390

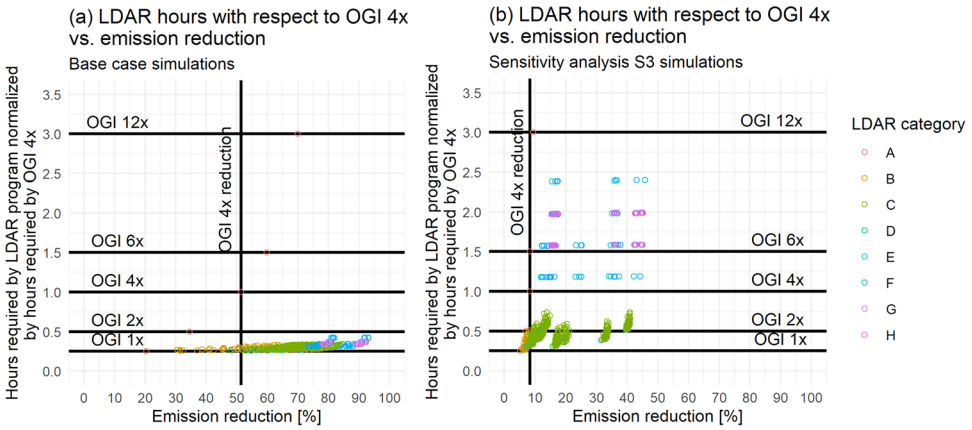

Figure 5. Number of hours required by LDAR programs normalized by the hours required by OGI 4× vs their emission reduction for (a) base case (long duration of high-emitters) and (b) sensitivity analysis S3 (short duration of high-emitters) simulations. The data points are colored by LDAR category: "A" = OGI, "B" = aerial + OGI, "C" = satellite + aerial + OGI, "D" = satellite + OGI, "E" = continuous + OGI, "F" = satellite + continuous + OGI, "G" = satellite + continuous at priority sites + OGI, and "H" = satellite + continuous at priority sites + aerial at non-priority sites + OGI. Horizontal black lines indicate the number of visits of OGI-only LDAR programs. The vertical black line indicates the reduction of OGI 4×. Each data point corresponds to one scenario in a particular LDAR category, with differences in detection threshold, frequency of inspections, and repair times.

types D vs E on Figure 4) and, thus, strategies that have continuous monitoring sensors located only at facilities with equipment prone to be high-emitting are equally effective. Overall, given that emissions can be found on a continuous basis, the time that larger leaks are emitting is decreased significantly and higher reductions than OGI 12× can be achieved.

NUMBER OF LDAR HOURS REQUIRED

In addition to evaluating emission reduction, the time needed to carry out the LDAR programs was considered in the analysis, including ground inspection, administrative, and driving hours. The approach is similar to the one described by Sridharan et al.[37] and is detailed in SI Section S10. Figure 5 shows the number of hours required in each LDAR program normalized by the hours needed in the OGI 4× program (also shown in Figures S14 and S15 in separate sub-plots for each LDAR type for more clarity). All simulations in the base case scenarios (Figure 5a) using advanced detection technologies lead to less time needed than OGI 2×, suggesting that many LDAR programs can achieve high emission reductions and be less labor intensive. However, when the duration of high-emitters is short, the number of site visits can increase significantly (Figure 5b). For sensitivity analysis S3, all scenarios of LDAR with aerial + OGI or satellite + aerial + OGI require less hours than 4× OGI, while those that incorporate continuous monitoring require more hours than OGI 4×. The detection threshold of continuous monitors is inversely proportional to the LDAR hours required as those with lower detection threshold require more time (Figure S12). Figure S13 shows the number of site visits required for sensitivity analysis S4 and S5 scenarios. The duration of high-emitters is a sensitive parameter for both the LDAR required hours and for emission reduction (Figures 5 and S13).

IMPLICATIONS AND MODEL LIMITATIONS

LDAR models like the one used in this work can effectively compare LDAR programs on a relative basis and have large uncertainty on predicting absolute emission reductions given the uncertainty in certain parameters. However, after varying key parameters in sensitivity analyses, consistent results evidence that LDAR strategies that combine detection technologies with a focus on finding and fixing the largest emissions quickly while having less frequent OGI inspections lead to greater reductions than strategies with only OGI surveys at intervals of months. Multiple combinations of technologies achieve larger reductions than OGI 4× or even OGI 12×, giving operators multiple options to choose from. These results are specific for oil and gas production basins where the contribution of emissions above 100 kg/h is 40−80% of production site-wide total emissions and could differ in basins with lower contribution from emissions above this threshold.

One assumption of LDAR models is that the leak generation rates are constant throughout the simulation due to limited data on leak recurrence, in particular for high-emitters. Variations in times of leak recurrence or absence of leak recurrence might occur due to equipment upgrades, replacements, or preventive maintenance. These practices were not implemented in this work; however, they would lead to further emission reductions than those reported here (see SI Section S11). In addition, operational changes such as reducing routine flaring would lead to higher reductions. While these practices were not implemented in the simulations, recent empirical studies suggest that effective reductions can be achieved by LDAR in the oil and gas production sector[29,38−40] and that methane emission intensity has been decreasing in the Permian Basin as a whole[41] and for some operators.[42] There is also lack of data on the temporal characteristics of high-emitters, which is a very sensitive parameter. Future work should focus on obtaining information on duration of high-emitters and on root-cause analysis, which will be particularly relevant when doing LDAR modeling coupled with a process-based simulator (like the MEET model) that includes routine emissions and with a finer simulation temporal resolution. Including routine emissions in the simulation might impact reduction as longer times might be needed to distinguish routine vs non-routine sources and might lead to more LDAR hours required in case operators are dispatched to sites due to routine sources. Emissions from gathering pipelines were not included in this work since this model does simulations for individual facilities and not over a particular geographic area coupled with atmospheric dispersion models. Recent evidence suggests that this source can be significant in some regions[8,43] and novel technologies, in particular remote sensing platforms, are helpful to detecting

https://doi.org/10.1021/acs.est.2c08582
Environ. Sci. Technol. 2023, 57, 7382−7390

these emissions. Recent studies show larger emissions than the distribution from non-routine emissions in the Permian here used but do not distinguish if they are leaks or routine short-duration emissions;[8,16] if some of these larger emissions were unintended, the distribution would be more skewed, leading to even more reductions with the combinations of advanced technologies.

■ ASSOCIATED CONTENT

Supporting Information

The Supporting Information is available free of charge at https://pubs.acs.org/doi/10.1021/acs.est.2c08582.

Detailed data on simulations conditions and additional graphs; Code and modeling data available at Zenodo via DOI 10.5281/zenodo.7853609 (PDF)

■ AUTHOR INFORMATION

Corresponding Author

Felipe J. Cardoso-Saldaña − *ExxonMobil Technology and Engineering Company, Spring, Texas 77389, United States;* orcid.org/0000-0002-6359-8076; Email: felipe.j.saldana@exxonmobil.com

Complete contact information is available at: https://pubs.acs.org/10.1021/acs.est.2c08582

Notes

The author declares no competing financial interest.

■ ACKNOWLEDGMENTS

Funding to perform the analyses reported here was provided by ExxonMobil Upstream Research Company. The author thanks Sam Aminfard for valuable comments.

■ REFERENCES

(1) IPCC, 2021: Summary for Policymakers. In *Climate Change 2021: The Physical Science Basis. Contribution of Working Group I to the Sixth Assessment Report of the Intergovernmental Panel on Climate Change*, Masson-Delmotte, V., Zhai, P., Pirani, A., Connors, S. L., Péan, C., Berger, S., Caud, N., Chen, Y., Goldfarb, L., Gomis, M. I., Huang, M., Leitzell, K., Lonnoy, E., Matthews, J. B. R., Maycock, T. K., Waterfield, T., Yelekçi, O., Yu, R., Zhou, B., Eds.; Cambridge University Press: Cambridge, United Kingdom and New York, NY, USA, 2021; pp 3−32.

(2) Global Methane Pledge. https://www.globalmethanepledge.org/ (Accessed September 1, 2022).

(3) Saunois, M.; Stavert, A. R.; Poulter, B.; Bousquet, P.; Canadell, J. G.; Jackson, R. B.; Zhuang, Q. The global methane budget 2000−2017. *Earth Syst. Sci. Data* **2020**, *12*, 1561−1623.

(4) Oil and Gas Climate Initiative (OGCI). Reducing methane emissions. https://www.ogci.com/action-and-engagement/reducing-methane-emissions/ (Accessed September 20, 2022).

(5) Brandt, A. R.; Heath, G. A.; Cooley, D. Methane leaks from natural gas systems follow extreme distributions. *Environ. Sci. Technol.* **2016**, *50*, 12512−12520.

(6) Alvarez, R. A.; Zavala-Araiza, D.; Lyon, D. R.; Allen, D. T.; Barkley, Z. R.; Brandt, A. R.; Hamburg, S. P. Assessment of methane emissions from the US oil and gas supply chain. *Science* **2018**, *361*, 186−188.

(7) Allen, D. T.; Torres, V. M.; Thomas, J.; Sullivan, D. W.; Harrison, M.; Hendler, A.; Seinfeld, J. H. Measurements of methane emissions at natural gas production sites in the United States. *Proc. Natl. Acad. Sci. U. S. A.* **2013**, *110*, 17768−17773.

(8) Cusworth, D. H.; Duren, R. M.; Thorpe, A. K.; Olson-Duvall, W.; Heckler, J.; Chapman, J. W.; Miller, C. E. Intermittency of large methane emitters in the Permian Basin. *Environ. Sci. Technol. Lett.* **2021**, *8*, 567−573.

(9) U.S. Environmental Protection Agency. *Oil and Natural Gas Sector: Emission Standards for New, Reconstructed, and Modified Sources*, 2016. https://www.regulations.gov/document/EPA-HQ-OAR-2010-0505-7562 (Accessed November 3, 2022).

(10) Fox, T. A.; Barchyn, T. E.; Risk, D.; Ravikumar, A. P.; Hugenholtz, C. H. A review of close-range and screening technologies for mitigating fugitive methane emissions in upstream oil and gas. *Environ. Res. Lett.* **2019**, *14*, No. 053002.

(11) Kemp, C. E.; Ravikumar, A. P.; Brandt, A. R. Comparing natural gas leakage detection technologies using an open-source "virtual gas field" simulator. *Environ. Sci. Technol.* **2016**, *50*, 4546−4553.

(12) Fox, T. A.; Gao, M.; Barchyn, T. E.; Jamin, Y. L.; Hugenholtz, C. H. An agent-based model for estimating emissions reduction equivalence among leak detection and repair programs. *J. Cleaner Prod.* **2021**, *282*, No. 125237.

(13) Kemp, C. E.; Ravikumar, A. P. New Technologies Can Cost Effectively Reduce Oil and Gas Methane Emissions, but Policies Will Require Careful Design to Establish Mitigation Equivalence. *Environ. Sci. Technol.* **2021**, *55*, 9140−9149.

(14) Zavala-Araiza, D.; Alvarez, R. A.; Lyon, D. R.; Allen, D. T.; Marchese, A. J.; Zimmerle, D. J.; Hamburg, S. P. Super-emitters in natural gas infrastructure are caused by abnormal process conditions. *Nat. Commun.* **2017**, *8*, 14012.

(15) Chen, Y.; Sherwin, E. D.; Berman, E. S.; Jones, B. B.; Gordon, M. P.; Wetherley, E. B.; Brandt, A. R. Quantifying Regional Methane Emissions in the New Mexico Permian Basin with a Comprehensive Aerial Survey. *Environ. Sci. Technol.* **2022**, *56*, 4317−4323.

(16) Irakulis-Loitxate, I.; Guanter, L.; Liu, Y. N.; Varon, D. J.; Maasakkers, J. D.; Zhang, Y.; Jacob, D. J. Satellite-based survey of extreme methane emissions in the Permian basin. *Sci. Adv.* **2021**, *7*, No. eabf4507.

(17) Sherwin, E.; Rutherford, J.; Zhang, Z.; Chen, Y.; Wetherley, E.; Yakovlev, P.; Cusworth, D. *Quantifying oil and natural gas system emissions using one million aerial site measurements*, 2023. https://doi.org/10.21203/rs.3.rs-2406848/v1 (Accessed February 27, 2023).

(18) Allen, D. T.; Cardoso-Saldaña, F. J.; Kimura, Y.; Chen, Q.; Xiang, Z.; Zimmerle, D.; Harrison, M. A Methane Emission Estimation Tool (MEET) for predictions of emissions from upstream oil and gas well sites with fine scale temporal and spatial resolution: Model structure and applications. *Sci. Total Environ.* **2022**, *829*, No. 154277.

(19) Zimmerle, D.; Duggan, G.; Vaughn, T.; Bell, C.; Lute, C.; Bennett, K.; Allen, D. T. Modeling air emissions from complex facilities at detailed temporal and spatial resolution: The Methane Emission Estimation Tool (MEET). *Sci. Total Environ.* **2022**, *824*, No. 153653.

(20) Stokes, S.; Tullos, E.; Morris, L.; Cardoso-Saldaña, F. J.; Smith, M.; Conley, S.; Allen, D. T. Reconciling Multiple Methane Detection and Quantification Systems at Oil and Gas Tank Battery Sites. *Environ. Sci. Technol.* **2022**, *56*, 16055−16061.

(21) Allen, D. T.; Cardoso-Saldaña, F. J.; Kimura, Y. Variability in spatially and temporally resolved emissions and hydrocarbon source fingerprints for oil and gas sources in shale gas production regions. *Environ. Sci. Technol.* **2017**, *51*, 12016−12026.

(22) Bell, C. S.; Vaughn, T. L.; Zimmerle, D.; Herndon, S. C.; Yacovitch, T. I.; Heath, G. A.; Soltis, J. Comparison of methane emission estimates from multiple measurement techniques at natural gas production pads. *Elementa: Sci. Anthropocene* **2017**, *5*, 79.

(23) Kuo, J.; Hicks, T. C.; Drake, B.; Chan, T. F. Estimation of methane emission from California natural gas industry. *J. Air Waste Manage. Assoc.* **2015**, *65*, 844−855.

(24) Pacsi, A. P.; Ferrara, T.; Schwan, K.; Tupper, P.; Lev-On, M.; Smith, R.; Ritter, K. Equipment leak detection and quantification at 67 oil and gas sites in the Western United States. *Elementa: Sci. Anthropocene* **2019**, *7*, 29.

(25) U.S. Environmental Protection Agency. *Standards of Performance for New, Reconstructed, and Modified Sources and Emissions Guidelines for Existing Sources: Oil and Natural Gas Sector Climate Review*, 2016. https://www.regulations.gov/docket/EPA-HQ-OAR-2021-0317 (Accessed January 2, 2022).

(26) Johnson, M. R.; Tyner, D. R.; Szekeres, A. J. Blinded evaluation of airborne methane source detection using Bridger Photonics LiDAR. *Remote Sens. Environ.* **2021**, *259*, No. 112418.
(27) Conrad, B. M.; Tyner, D. R.; Johnson, M. R. Robust probabilities of detection and quantification uncertainty for aerial methane detection: Examples for three airborne technologies. *Remote Sens. Environ.* **2023**, *288*, No. 113499.
(28) City of Fort Worth Natural Gas Air Quality Study Final Report (2011). Prepared by Eastern Research Group, Inc. and Sage Environmental Consulting, LP for City of Fort Worth. https://www.fortworthtexas.gov/files/assets/public/development-services/documents/gaswells/air-quality-study-final.pdf (Accessed August 1, 2022).
(29) Ravikumar, A. P.; Roda-Stuart, D.; Liu, R.; Bradley, A.; Bergerson, J.; Nie, Y.; Brandt, A. R. Repeated leak detection and repair surveys reduce methane emissions over scale of years. *Environ. Res. Lett.* **2020**, *15*, No. 034029.
(30) Environmental Defense Fund. *PermianMap, Flaring Aerial Survey Results*, 2022. https://www.permianmap.org/flaring-emissions/ (Accessed August 1, 2022).
(31) Zimmerle, D.; Vaughn, T.; Bell, C.; Bennett, K.; Deshmukh, P.; Thoma, E. Detection limits of optical gas imaging for natural gas leak detection in realistic controlled conditions. *Environ. Sci. Technol.* **2020**, *54*, 11506−11514.
(32) U.S. Environmental Protection Agency. *Standards of Performance for New, Reconstructed, and Modified Sources and Emissions Guidelines for Existing Sources: Oil and Natural Gas Sector Climate Review*, 2022. https://www.regulations.gov/document/EPA-HQ-OAR-2021-0317-1460 (Accessed August 1, 2022).
(33) Jacob, D. J.; Varon, D. J.; Cusworth, D. H.; Dennison, P. E.; Frankenberg, C.; Gautam, R.; Duren, R. M. Quantifying methane emissions from the global scale down to point sources using satellite observations of atmospheric methane. *Atmos. Chem. Phys.* **2022**, *22*, 9617−9646.
(34) Millward, J. *How Methane Detection Space Tech Can Play a Role in Methane Detection to Impact Climate Change Via Satellite*, 2022. https://www.satellitetoday.com/opinion/2022/05/26/how-methane-detection-space-tech-can-play-a-role-in-methane-detection-to-impact-climate-change/ (Accessed September 20, 2022).
(35) Chen, Q.; Modi, M.; McGaughey, G.; Kimura, Y.; McDonald-Buller, E.; Allen, D. T. Simulated Methane Emission Detection Capabilities of Continuous Monitoring Networks in an Oil and Gas Production Region. *Atmosphere* **2022**, *13*, 510.
(36) Ravikumar, A.P. *FEAST: US − Alternative LDAR programs for representative US O&G Production Facilities. Comment to US Environmental Protection Agency submitted by Environmental Defense Fund, Attachment L − FEAST National Slides*, 2022. https://www.regulations.gov/comment/EPA-HQ-OAR-2021-0317-0844 (Accessed August 1, 2022).
(37) Sridharan, S.; Lazarus, A.; Reese, C.; Wetherley, E.; Bushko, K.; Berman, E. Long Term, Periodic Aerial Surveys Cost Effectively Mitigate Methane Emissions. In *SPE Annual Technical Conference and Exhibition*; OnePetro, 2020.
(38) Wang, J.; Barlow, B.; Funk, W.; Robinson, C.; Brandt, A. R.; Ravikumar, A. *Large-Scale Controlled Experiment Demonstrates Effectiveness of Methane Leak Detection and Repair Programs at Oil and Gas Facilities*, 2021. https://eartharxiv.org/repository/view/2935/ (Accessed August 1, 2022).
(39) Johnson, F.; Wlazlo, A.; Keys, R.; Desai, V.; Wetherley, E. B.; Calvert, R.; Berman, E. S. *Airborne methane surveys pay for themselves: An economic case study of increased revenue from emissions control*, 2021. https://eartharxiv.org/repository/view/2532/ (Accessed August 1, 2022)
(40) Cheadle, L. C.; Tran, T.; Nyarady, J. F.; Lozo, C. Leak detection and repair data from California's oil and gas methane regulation show decrease in leaks over two years. *Environ. Challenges* **2022**, *8*, No. 100563.
(41) Varon, D. J.; Jacob, D. J.; Hmiel, B.; Gautam, R.; Lyon, D. R.; Omara, M.; Aben, I. Continuous weekly monitoring of methane emissions from the Permian Basin by inversion of TROPOMI satellite observations. *Atmos. Chem. Phys. Discuss.* **2022**, 1−26.
(42) Hmiel, B.; Lyon, D. R.; Warren, J. D.; Yu, J.; Cusworth, D. H.; Duren, R. M.; Hamburg, S. P. Empirical quantification of methane emission intensity from oil and gas producers in the Permian basin. *Environ. Res. Lett.* **2023**, *18*, No. 024029.
(43) Cusworth, D.; Thorpe, A.; Ayasse, A.; Stepp, D.; Heckler, J.; Asner, G.; Duren, R. Strong methane point sources contribute a disproportionate fraction of total emissions across multiple basins in the US. *Proc. Natl. Acad. Sci. U. S. A.* **2022**, *119*, No. e2202338119.

https://doi.org/10.1021/acs.est.2c08582
Environ. Sci. Technol. 2023, 57, 7382−7390